

# Investigation of the Interface Traps and Current Collapse in LPCVD SiN<sub>x</sub>/AlGa<sub>0.7</sub>N/GaN MISHEMTs

Kun Yu<sup>1</sup>, Chao Liu<sup>2</sup>, Huaxing Jiang<sup>2</sup>, Xing Lu<sup>1</sup>, Kei May Lau<sup>2</sup> and Anping Zhang<sup>1</sup>

<sup>1</sup>State Key Laboratory of Electrical Insulation and Power Equipment, Xi'an Jiaotong University, Xi'an, China  
E-mail: [exlu@connect.ust.hk](mailto:exlu@connect.ust.hk) Phone: +86 8266 4008

<sup>2</sup>Department of Electronic and Computer Engineering, Hong Kong University of Science and Technology, Hong Kong, China

**Keywords:** AlGa<sub>0.7</sub>N/GaN MISHEMTs, Current collapse, Interface traps, LPCVD SiN<sub>x</sub>, Pulsed I-V

## Abstract

We report on a study of AlGa<sub>0.7</sub>N/GaN metal-insulator-semiconductor high electron mobility transistors (MISHEMTs) using low pressure chemical vapor deposition (LPCVD) SiN<sub>x</sub> as the gate dielectric and plasma enhanced chemical vapor deposition (PECVD) SiN<sub>x</sub> as the further passivation layer. The interface traps and current collapse in the devices were investigated by means of pulsed I-V measurements. The OFF-to-ON switching tests revealed that a bilayer LPCVD SiN<sub>x</sub>/PECVD SiN<sub>x</sub> passivation scheme is distinctly effective for suppressing the current collapse.

## INTRODUCTION

GaN-based metal-insulator-semiconductor high electron mobility transistors (MISHEMTs) have attracted great attraction for power switching and RF applications owing to their superior properties such as high breakdown voltage and high electron mobility. In order to enhance the MISHEMTs' gate control capability and operation stability, most recent development has focused on the gate dielectric preparation and the following dielectric/III-nitride interface quality issues. Significant progress has been made on MISHEMTs using SiN<sub>x</sub> grown by plasma enhanced chemical vapor deposition (PECVD) or *in-situ* metal-organic chemical vapor deposition (MOCVD) [1, 2]. However, simultaneous realization of low gate leakage, large gate swing, low current collapse and high gate stability is still challenging. Very recently, low pressure chemical vapor deposition (LPCVD) SiN<sub>x</sub> has been explored as a promising gate dielectric and passivation material for AlGa<sub>0.7</sub>N/GaN MISHEMTs due to its high temperature and plasma-free deposition process, which can lead to high film quality and less damage on the AlGa<sub>0.7</sub>N barrier [3, 4]. In this work, we performed a thorough study of the interface traps and current collapse in LPCVD SiN<sub>x</sub>/AlGa<sub>0.7</sub>N/GaN MISHEMTs using pulsed I-V measurements. It was revealed that the current collapse of the MISHEMTs could be effectively suppressed by a LPCVD SiN<sub>x</sub>/PECVD SiN<sub>x</sub> bilayer passivation scheme.

## DEVICE FABRICATION

The AlGa<sub>0.7</sub>N/GaN heterostructures used in this study were grown by MOCVD on a 2-in. sapphire substrate. The epilayers consist of, from bottom to top, a 3- $\mu$ m GaN buffer layer, a 1-nm AlN spacer layer and a 20-nm Al<sub>0.3</sub>Ga<sub>0.7</sub>N barrier layer. The LPCVD SiN<sub>x</sub>/AlGa<sub>0.7</sub>N/GaN MISHEMT structure was schematically shown in Fig. 1.

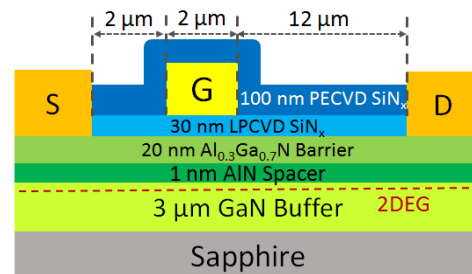


Fig. 1. Schematic diagram of the LPCVD SiN<sub>x</sub>/AlGa<sub>0.7</sub>N/GaN MISHEMT.

Device fabrication started from mesa isolation by a Cl<sub>2</sub>-based inductively coupled plasma (ICP) dry etching. Then, three cycles of a digital etching process were performed immediately prior to the deposition of SiN<sub>x</sub> by LPCVD. Each digital etching process began with UV/Ozone oxidation for 3 min and stopped with dilute hydrochloric acid (H<sub>2</sub>O:HCl = 5:1) etching for 1 min. As the gate dielectric, 30 nm LPCVD SiN<sub>x</sub> was deposited at 800 °C with a NH<sub>3</sub> flow of 50 sccm and a SiH<sub>2</sub>Cl<sub>2</sub> flow of 16 sccm. The pressure in the LPCVD chamber is 200 mTorr and the deposition rate is about 3.3 nm/min. To prevent the GaN decomposition, NH<sub>3</sub> was imported into the chamber during the heating process before deposition.

After opening the contact holes, the source/drain Ohmic contacts were formed by e-beam evaporation of Ti/Al/Ni/Au based metal stack and a lift-off process, followed by an 850 °C anneal for 30 s in a nitrogen ambient. The gate metal was Ni/Au and the device was further passivated using 100 nm PECVD SiN<sub>x</sub>. To make comparison, a control MISHEMT sample without PECVD SiN<sub>x</sub> passivation was also prepared.

The MISHEMTs discussed in this paper featured a gate length ( $L_G$ ) of 2  $\mu$ m, a gate width ( $W_G$ ) of 10  $\mu$ m, a gate-to-

drain distance ( $L_{GD}$ ) of 12  $\mu\text{m}$  and a gate-to-source distance ( $L_{GS}$ ) of 2  $\mu\text{m}$ .

## RESULTS AND DISCUSSION

Fig. 2 compares the DC output and transfer characteristics of the LPCVD  $\text{SiN}_x/\text{AlGaIn}/\text{GaIn}$  MISHEMTs with and without PECVD  $\text{SiN}_x$  passivation. The maximum drain current densities of both devices are around 1 A/mm at  $V_{DS} = 15$  V and  $V_{GS} = 2$  V (Fig. 2(a)). Compared with the MISHEMT without PECVD  $\text{SiN}_x$  passivation, the bilayer passivated device exhibited negligible hysteresis in the double-mode transfer characteristics (Fig. 2(b)). This could be attributed to the suppression of trap states that located at the MISHEMTs' access region by the PECVD  $\text{SiN}_x$  passivation.

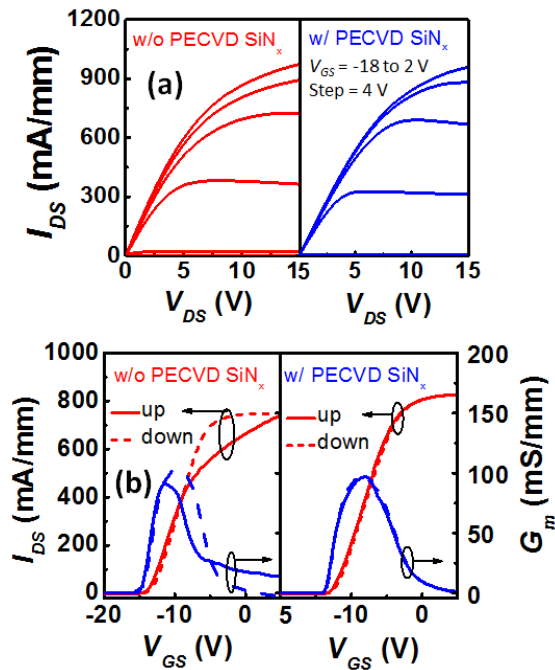


Fig. 2. (a) DC output and (b) double-mode transfer characteristics of the LPCVD  $\text{SiN}_x/\text{AlGaIn}/\text{GaIn}$  MISHEMTs.

According to Fig. 3, the LPCVD  $\text{SiN}_x/\text{AlGaIn}/\text{GaIn}$  MISHEMTs exhibited a very low gate leakage of  $10^{-8}$  A/cm<sup>2</sup> at a reverse bias of -20 V and a large gate swing up to +20 V, implying the high quality of the LPCVD  $\text{SiN}_x$  film.

The interface trap state density of the LPCVD  $\text{SiN}_x/\text{AlGaIn}/\text{GaIn}$  MISHEMTs was analyzed using pulsed  $I_{DS}-V_{GS}$  method [5]. The pulse width ( $W_p$ ) and pulse period ( $P_p$ ) were 5  $\mu\text{s}$  and 100 ms, respectively.  $V_{DS}$  was kept at a low value of 2 V, in order to maintain a nearly uniform occupancy of the interface traps in the gate region. In Fig. 4, the up-sweep pulsed  $I_{DS}-V_{GS}$  curve with low  $V_{GS\_base}$  of -15 V was regarded as a baseline with minimal electron trapping in interface

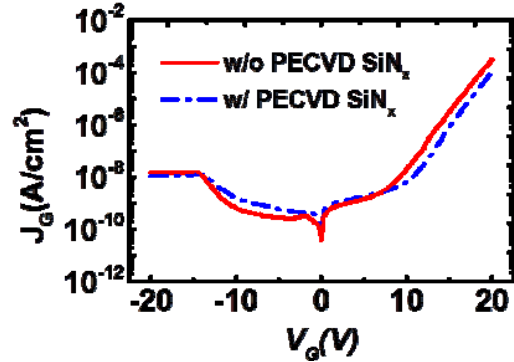


Fig. 3. Gate leakage curves of the LPCVD  $\text{SiN}_x/\text{AlGaIn}/\text{GaIn}$  MISHEMTs.

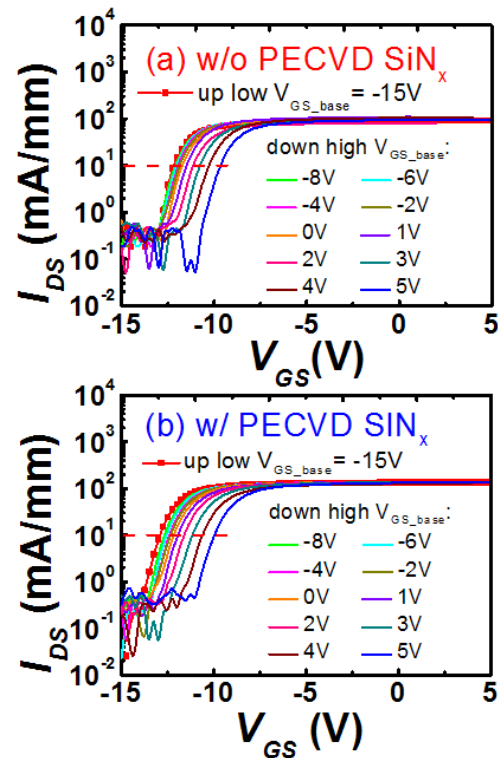


Fig. 4. Pulse-mode  $I_{DS}-V_{GS}$  characteristics at  $V_{DS} = 2$  V. The pulse width and pulse period are 5  $\mu\text{s}$  and 100 ms, respectively.

states. In the down sweep, a high  $V_{GS\_base}$  was aimed at filling up the interface states below the Fermi level corresponding to the high  $V_{GS\_base}$ , resulting in the hysteresis of the pulsed  $I_{DS}-V_{GS}$  curve. Interface states with time constants shorter than  $W_p = 5\mu\text{s}$  would emit electrons before each measurement point and thus could not be detected using this pulsed  $I_{DS}-V_{GS}$  method. The detectable energy range could be deduced from the Shockley-Read-Hall statistics

$$\tau_e = \frac{1}{v_{th}\sigma_n N_C} \exp\left(\frac{E_C - E_T}{kT}\right) \quad (1)$$

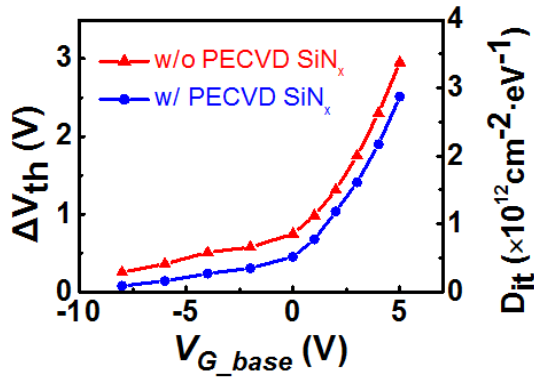


Fig. 5.  $\Delta V_{th}$  and  $D_{it}$  extracted from the pulse mode  $I_{DS}-V_{GS}$  measurements.

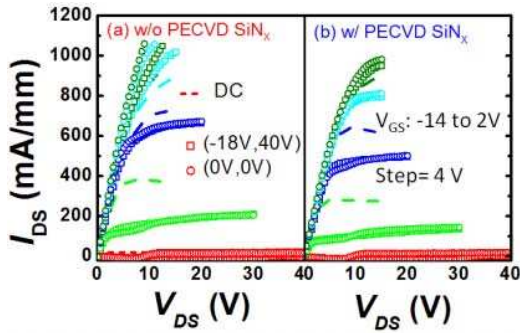


Fig. 6. Pulsed  $I_{DS}-V_{DS}$  characteristics (with the DC reference) measured from two quiescent bias points of  $(V_{GSQ}, V_{DSQ}) = (-18 \text{ V}, 40 \text{ V})$  and  $(0 \text{ V}, 0 \text{ V})$ .

where  $v_{th}$ ,  $\sigma_n$  and  $N_C$  are the electron thermal velocity, electron capture cross section and electron concentration at the effective density of states in the conduction band in GaN, respectively [5, 6]. In this work, the detectable energy range was calculated to be  $E_C - E_T \geq 0.38 \text{ eV}$ .

The interface trap density  $D_{it}$  could be determined by

$$D_{it} = \frac{C_{OX} \cdot \Delta V_{TH}}{q^2} \quad (2)$$

where  $C_{OX} = 192 \text{ nF/cm}^2$ , and  $\Delta V_{TH}$  is the hysteresis extracted from the pulsed  $I_{DS}-V_{GS}$  curves in Fig. 4.

Fig. 5 plots the hysteresis and the interface trap state density as a function of  $V_{GS\_base}$ . The small difference of  $D_{it}$  between the MISHEMTs with and without PECVD  $\text{SiN}_x$  passivation suggested that the PECVD  $\text{SiN}_x$  layer has less influence on the trap states in the MISHEMTs' gate region.

To further evaluate the current collapse quantitatively, pulsed  $I_{DS}-V_{DS}$  measurements were performed for both samples [7]. Fig. 6 illustrates the pulsed  $I_{DS}-V_{DS}$  curves measured from two quiescent bias conditions of  $(V_{GSQ}, V_{DSQ}) = (-18 \text{ V}, 40 \text{ V})$  and  $(0 \text{ V}, 0 \text{ V})$ . The negligible difference observed in the linear region of the pulsed  $I_{DS}-V_{DS}$  curves for the bilayer  $\text{SiN}_x$  passivated MISHEMT suggested a low current collapse, while the unpassivated device showed obvious current collapse.

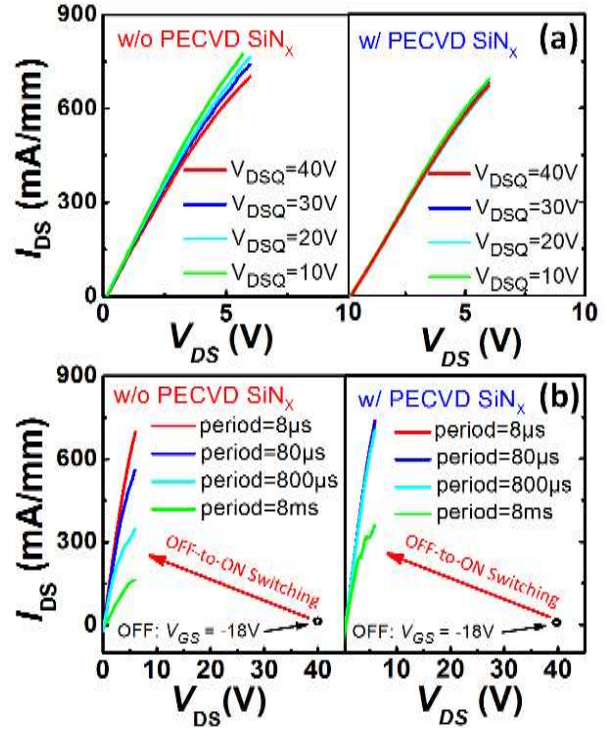


Fig. 7. OFF-to-ON switching tests with various OFF-state  $V_{DSQ}$  (a) stress from 10 to 40 V and (b) stress period from 8  $\mu\text{s}$  to 8 ms.

The transient OFF-to-ON switching characterizations were performed for the fabricated MISHEMTs. As shown in Fig. 7(a), the devices were switched from the OFF state with a quiescent gate bias of  $-18 \text{ V}$  and a quiescent drain bias of  $10\text{--}40 \text{ V}$  ( $10 \text{ V}$  step) to the ON state with a gate bias of  $2 \text{ V}$ . The applied pulse width and period are  $0.8 \mu\text{s}$  and  $8 \mu\text{s}$ , respectively. Dynamic  $R_{ON}$  was extracted from the linear regime ( $V_{DS}$ : 0 to 6 V) of the pulsed output curve. For the passivated MISHEMT, the pulsed output curves with various OFF-state drain biases were highly overlapped, while evident dispersion was observed among the curves for the unpassivated device.

Fig. 7(b) shows the pulsed output curves under a 40-V OFF-state drain bias with various OFF-state  $V_{DSQ}$  stress periods from  $8 \mu\text{s}$  to 8 ms. For the passivated MISHEMT, the dynamic  $R_{ON}$  with a stress period of  $800 \mu\text{s}$  remained as low as only 1.04 times of the one with a stress period of  $8 \mu\text{s}$ . By contrast, the ratio with the same measurement conditions for the unpassivated device was 2.10. In addition, the passivated MISHEMT exhibited much lower dynamic  $R_{ON}$  degradation even with a stress period of 8 ms. The low current collapse in the bilayer  $\text{SiN}_x$  passivated MISHEMT could be attributed to the shallow donor-like traps existing at the  $\text{SiN}_x/\text{III-Nitride}$  interface, which could modify the surface potential and inhibit electron injection from gate into surface states [8, 9].

## CONCLUSIONS

We have investigated the interface traps and current collapse in LPCVD SiN<sub>x</sub>/AlGaIn/GaN MISHEMTs. Small gate leakage current, large gate swing and low interface trap state density demonstrated the feasibility of using LPCVD SiN<sub>x</sub> as gate dielectric for AlGaIn/GaN MISHEMTs. Moreover, an LPCVD SiN<sub>x</sub>/PECVD SiN<sub>x</sub> bilayer passivation scheme has been developed for the MISHEMTs to suppress the current collapse, leading to enhanced dynamic performance.

## REFERENCES

- [1] X. Hu, A. Koudymov, G. Simin, J. Yang, M. A. Khan, A. Tarakji, M. S. Shur and R. Gaska (2001) 'Si<sub>3</sub>N<sub>4</sub>/AlGaIn/GaN-metal-insulator-semiconductor heterostructure field-effect transistors', *Applied Physics Letters*, 79(17), pp. 2832.
- [2] X. Lu, J. Ma, H. Jiang, C. Liu and K. M. Lau (2014) 'Low trap states in in-situ SiN<sub>x</sub>/AlIn/GaN metal-insulator-semiconductor structures grown by metal-organic chemical vapor deposition', *Applied Physics Letters*, 105(10), pp. 102911.
- [3] M. Hua, C. Liu, S. Yang, S. Liu, K. Fu, Z. Dong, Y. Cai, B. Zhang and K. J. Chen (2015) 'GaN-Based Metal-Insulator-Semiconductor High-Electron-Mobility Transistors Using Low-Pressure Chemical Vapor Deposition SiN<sub>x</sub> as Gate Dielectric', *IEEE Electron Device Letters*, 36(5), pp. 448-450.
- [4] X. H. Wang, S. Huang, Y. K. Zheng, K. Wei, X. J. Chen, G. G. Liu, T. T. Yuan, W. J. Luo, L. Pang, H. J. Jiang, J. F. Li, C. Zhao, H. X. Zhang and X. Y. Liu (2015) 'Robust SiN<sub>x</sub>/AlGaIn Interface in GaN HEMTs Passivated by Thick LPCVD-Grown SiN<sub>x</sub> Layer', *Ieee Electron Device Letters*, 36(7), pp. 666-668.
- [5] S. Yang, S. Liu, Y. Lu, C. Liu and K. J. Chen (2015) 'AC-Capacitance Techniques for Interface Trap Analysis in GaN-Based Buried-Channel MIS-HEMTs', *IEEE Transactions on Electron Devices*, 62(6), pp. 1870-1878.
- [6] C. Mizue, Y. Hori, M. Miczek and T. Hashizume (2011) 'Capacitance-Voltage Characteristics of Al<sub>2</sub>O<sub>3</sub>/AlGaIn/GaN Structures and State Density Distribution at Al<sub>2</sub>O<sub>3</sub>/AlGaIn Interface', *Japanese Journal Of Applied Physics*, 50(2), pp. 021001.
- [7] Z. Tang, S. Huang and K. J. Chen 'Stability and Temperature Dependence of Dynamic RON in AlN-Passivated AlGaIn/GaN HEMT on Si Substrate', in CS MANTECH Conference, May. 2014, pp. 97-100.
- [8] Y. Ohno, T. Nakao, S. Kishimoto, K. Maezawa and T. Mizutani (2004) 'Effects of surface passivation on breakdown of AlGaIn/GaN high-electron-mobility transistors', *Applied physics letters*, 84(12), pp. 2184-2186.
- [9] M. Faqir, G. Verzellesi, A. Chini, F. Fantini, F. Danesin, G. Meneghesso, E. Zanoni and C. Dua (2008) 'Mechanisms of RF Current Collapse in AlGaIn-GaN High Electron Mobility Transistors', *IEEE Transactions on Device and Materials Reliability*, 8(2), pp. 240-247.

## ACRONYMS

MISHEMT: Metal-Insulator-Semiconductor High  
Electron Mobility Transistor

LPCVD: Low Pressure Chemical Vapor Deposition

PECVD: Plasma Enhanced Chemical Vapor Deposition

MOCVD: Metal-Organic Chemical Vapor Deposition

ICP: Inductively Coupled Plasma